bility of SIR-B, with its small R/V ratio, was substantially better than that of Seasat.

The practical utility of satellite-derived directional wave spectra (from either SAR or ROWS) for assimilation into operational wave models is reinforced by our results, although a low-altitude (<300 km) orbit will be necessary to achieve practical SAR imaging of azimuth-traveling waves. These results also indicate that the dominant wave number predicted by GSOWM was accurate but that the dominant wave direction was in disagreement with the independent estimates by about 30°.

REFERENCES AND NOTES

1. G. C. Ewing, Ed., *Oceanography from Space* (Woods Hole Oceanographic Institution Report NASA-CR-64164, Woods Hole, MA, 1965).
2. W. Alpers, *J. Geophys. Res.* **88**, 1745 (1983).
3. R. C. Beal *et al.*, *ibid.*, p. 1761.
4. R. C. Beal *et al.*, *ibid.*, in press.
5. K. Hasselmann *et al.*, *ibid.* **90**, 4659 (1985).
6. E. J. Walsh *et al.*, *J. Phys. Oceanogr.* **15**, 566 (1985).
7. F. C. Jackson, W. T. Walton, C. Y. Peng, *J. Geophys. Res.* **90**, 1005 (1985).
8. R. M. Clancy *et al.*, *Bull. Am. Meteorol. Soc.*, in press.
9. O. M. Phillips, in *Spaceborne Synthetic Aperture Radar for Oceanography*, R. C. Beal, P. S. DeLeonibus, I. Katz, Eds. (Johns Hopkins Press, Baltimore, 1981), p. 24.

10. We are indebted to the government of Chile for vital aircraft logistic and meteorological support, to the government of Argentina for alternate landing privileges, to the NASA P-3 crew for their precision underflights, and to the California Institute of Technology Jet Propulsion Laboratory SIR-B team for their dedicated mission support and timely SAR image-processing. This work was supported by the National Aeronautics and Space Administration and the Office of Naval Research.

5 August 1985; accepted 21 February 1986

*p*H-Induced Metabolic Transitions in *Artemia* Embryos Mediated by a Novel Hysteretic Trehalase

STEVEN C. HAND* AND JOHN F. CARPENTER†

Gastrula-stage embryos of the brine shrimp *Artemia* undergo reversible transitions between metabolically active and dormant states that are promoted by changes in intracellular *p*H. A macromolecular mechanism for this suppression of energy metabolism that involves regulation of the enzyme trehalase is reported here. Isolated trehalase from these embryos existed in two active forms that interconverted when exposed to physiological transitions in *p*H. This hysteretic interconversion was reversible, required minutes for completion, and involved a change in enzyme polymerization. The two states differed twofold in molecular size and were distinguishable electrophoretically. Compared to the smaller species, the polymerized form was strongly inhibited by acidic *p*H, adenosine 5′-triphosphate, and the substrate trehalose. Thus, the shift in assembly equilibrium toward the aggregated enzyme caused by *p*H values less than or equal to 7.4 may mediate the arrest of trehalose-fueled metabolism and respiration during dormancy in this cryptobiotic organism.

THE ROLE OF INTRACELLULAR *p*H (pH_i) in the suppression and activation of cellular metabolism is becoming increasingly well documented for both unicellular and multicellular organisms. Entry into and exit from dormancy is often accompanied by various amounts of acidification and alkalinization of the cellular milieu (*1*). In the brine shrimp *Artemia*, hydrated embryos (cysts) undergo reversible transitions between a metabolically active state of aerobic development and a cryptobiotic condition termed anaerobic dormancy (*2*); these transitions are accompanied by large shifts in pH_i from values of or above 7.9 to 6.3 (*3*). pH_i is the fundamental regulator for the transitions between these very different metabolic states (*4*). Acidification of the pH_i of aerobically developing cysts to 6.8 by exposure to elevated levels of CO_2 (aerobic acidosis) induces a quiescent condition comparable to anaerobic dormancy, as judged by suppression of hatching and oxygen consumption; removal of CO_2 reverses the effect. The mechanism by which this proton signal is coupled to the observed physiological response is the focus of our study.

In *Artemia* cysts, preemergence development and metabolism is fueled exclusively by the disaccharide trehalose (*5, 6*), and transitions in pH_i directly and reversibly arrest carbohydrate metabolism in these embryos (*7*). This evaluation (*7*) of carbohydrate levels with crossover point theory (*8*) revealed that the conversion of trehalose to glucose is the first nonequilibrium reaction reversibly inhibited by pH_i during both aerobic acidosis and anaerobic dormancy. If one assumes that all mobilized trehalose that is not converted to glycerol or glycogen is completely oxidized under aerobic conditions (*6*), the 95 percent shutdown of trehalose catabolism in aerobic acidosis (*7*) quantitatively accounts for the large suppression of oxygen consumption (*4*) seen under these conditions.

Thus, any mechanism proposed for the *p*H-induced metabolic transitions in *Artemia* embryos must explain the proton modulation of the trehalase reaction. We suggest that the proton-dependent shutdown of trehalose mobilization, and thereby energy metabolism, in these embryos results from a shift in assembly equilibrium of a novel, hysteretic trehalase. As originally defined (*9*), hysteretic enzymes have certain kinetic or molecular characteristics that respond slowly to a rapid change in the concentration of a ligand (for example, protons in the case of *Artemia* trehalase). The change in ligand concentration presumably induces a conversion of one enzyme form to another form that has different properties.

Our initial examination of crude trehalase preparations from hydrated cysts (Great Salt Lake, Utah, population) using nondenaturing polyacrylamide gel electrophoresis (PAGE) revealed two distinct, catalytically active forms of the enzyme (Fig. 1A) that could be visualized with substrate-specific activity staining (*10*). Multiple molecular species of trehalase are also seen in electrophoretic studies of the enzyme from insects and cellular slime mold (*11*). Elution profiles of *Artemia* trehalase activity from hydroxylapatite columns suggested that the two forms were interconvertible. We, therefore, separated this chromatographically enriched mixture of trehalase forms that exist at *p*H 7.0 (*12*) by electrophoresis on preparative slab gels, cut the slow-migrating form (which was well separated from the more mobile band) from the gel, and extracted it from the acrylamide matrix with buffer. Electrophoresis of the eluted trehalase on analytical gels again revealed the presence of both the slow- and fast-migrating forms (Fig. 1B) at the same ratio seen in the preparative gel; thus the slow-migrating molecular species could give rise to the fast-migrating form.

The first evidence suggesting that the molecular interconversion of trehalase was reversible and directly promoted by alter-

Department of Biology, University of Southwestern Louisiana, Lafayette, LA 70504.

*Present address: Department of Environmental, Population and Organismic Biology, University of Colorado, Boulder, CO 80309.
†Present address: Department of Zoology, University of California, Davis, CA 95616.

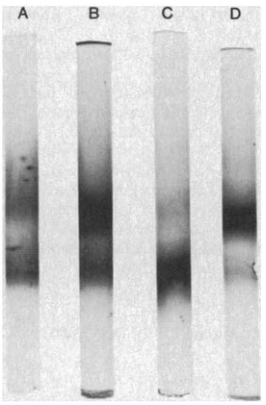

Fig. 1. Nondenaturing polyacrylamide gels showing the two molecular forms of trehalase from *Artemia* embryos. (A) Enzyme banding pattern observed in a crude extract (concentrated by ammonium sulfate precipitation). (B) The slow-migrating trehalase species, which had been separated from the faster form with preparative gels (see text), was dialyzed at *p*H 7.0, and reanalyzed with analytical PAGE as a test for interconversion of enzyme forms. (C) Gel of chromatographically enriched trehalase dialyzed overnight at *p*H 8.6. (D) The enzyme preparation in (C) at *p*H 8.6 was exposed to a second dialysis *p*H 6.3 and then electrophoresed as before.

ations in *p*H came from experiments in which we changed the *p*H of the chromatographically enriched trehalase preparation. This enzyme, which yielded the banding pattern seen in Fig. 1B when at *p*H 7.0, was dialyzed at *p*H 8.6 and then at *p*H 6.3. The treatment at *p*H 8.6 promoted a prominent shift in the ratio of trehalase forms toward the fast-migrating species (Fig. 1C); dialysis at *p*H 6.3 reversed the effect to increase the amount of the slow form (Fig. 1D). Direct titration of trehalase from *p*H 6.3 to 8.6, and observation of the electrophoretic pattern as a function of time at the new *p*H, indicated that the maximal shift in equilibrium toward the fast form was complete within 10 minutes. In contrast, maximal conversion to the slow-migrating species required more than an hour at *p*H 6.3.

To investigate the molecular basis for the *p*H-induced interconversion between electrophoretically distinct forms of *Artemia* trehalase, we dialyzed identical enzyme samples at either *p*H 6.3 or 8.6 and then chromatographed each on the same gel filtration column equilibrated with the respective buffer (50 m*M*) of appropriate *p*H (Fig. 2). The elution profiles for the two samples were different, and the protein standards (Fig. 2, inset) indicated a molecular weight of 235,000 for the enzyme at *p*H 6.3 (slow-migrating form) and 110,000 for the enzyme at *p*H 8.6 (fast-migrating form). The trehalase forms differed approximately twofold in molecular weight; these data are consistent with a mechanism whereby low *p*H fosters enzyme polymerization and alkaline values promote depolymerization. The quaternary structures of the two forms are not known, so descriptive terms referring to subunit composition (monomer, dimer, and tetramer) have not been applied.

Because hysteretic enzymes are important in metabolic regulation (*9, 13*), we determined whether physiologically relevant changes in trehalase kinetic properties occur as a result of shifts in assembly equilibrium. Using two different experimental approaches, we determined *p*H profiles of catalytic activity (*14*). First, a *p*H profile was generated by equilibrating individual enzyme samples for 4 hours at each experimental *p*H prior to assaying for activity at those respective *p*H values. This step allowed the enzyme to reach assembly equilibrium before analysis. In the second approach, the enzyme was shifted to the dissociated form by dialysis at *p*H 8.6 overnight. A *p*H profile was then determined without allowing any pre-equilibration prior to catalytic assay at a given *p*H. Because repolymerization of trehalase is quite slow, relatively little reassociation would occur during the 5-minute assays, even at low *p*H values. Thus, this profile would reflect the kinetic response of the depolymerized enzyme to *p*H. However, the rapid kinetics of trehalase depolymerization precluded our obtaining an accurate *p*H profile of the fully polymerized enzyme. Comparison of the *p*H profiles of the two forms (Fig. 3), indicated that *Artemia* trehalase becomes more *p*H-sensitive as the degree of enzyme assembly increases, that is, at lower *p*H values. Furthermore, the *p*H at which the two curves began to diverge (*p*H 7.4) indicated the point at which enzyme polymerization begins.

By taking advantage of the large difference in catalytic activity between the two curves at *p*H 7.0 (Fig. 3), we could gain a more accurate appraisal of the time dependency of trehalase assembly, as well as the capacity for reversal of the process. One would expect to see suppression of catalytic activity (measured at *p*H 7.0) as enzyme polymerization proceeds at acidic *p*H. Indeed, loss of trehalase activity after titration to *p*H 6.3 was exponential with time, and the majority of the inhibition occurred within 1 hour (Fig. 4A). Returning this polymerized enzyme to *p*H 8.6 by dialysis fully reversed the catalytic suppression (Fig. 4A, closed square). In the reciprocal experiment, where the polymerized enzyme (*p*H 6.3) was titrated to 8.6 to promote dissociation, catalytic activation was rapid and occurred within 5 minutes. The time required for hysteretic shifts in assembly equilibrium was comparable to that estimated in the electrophoretic experiments, and thus the process can be demonstrated by both catalytic and physical techniques.

Although the two polymerization states of trehalase clearly display different degrees of inhibition at acidic *p*H, other kinetic differences must exist if the observed shift in assembly equilibrium is to fully account for the shutdown of trehalose hydrolysis in cysts during anaerobic dormancy and aerobic acidosis. Our catalytic measurements at *p*H 6.8 demonstrated that *Artemia* trehalase is inhibited by adenosine 5′-triphosphate (ATP)

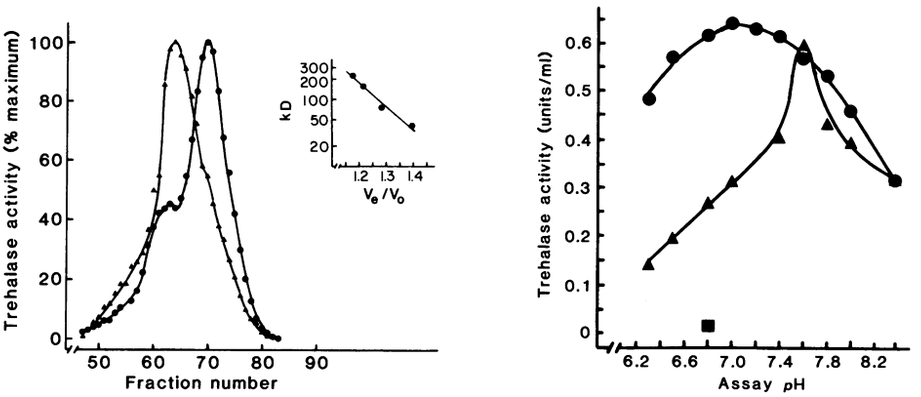

Fig. 2. (left). Elution profiles of trehalase at *p*H 6.3 (triangles) or *p*H 8.6 (circles) from a Sephacryl S-200 gel filtration column. Fractions were assayed for trehalase activity at *p*H 7.8. (Inset) The calibration curve for the column generated with proteins of known molecular weight (thyroglobulin, 669,000, for determination of exclusion volume; catalase, 232,000; aldolase, 158,000; transferrin, 74,000; ovalbumin, 41,000). Fig. 3. (right). Trehalase activity as a function of *p*H for enzyme that was either dialyzed at *p*H 8.6 (circles) or was pre-equilibrated at each individual assay *p*H for 4 hours prior to measurement of catalytic activity (triangles). The closed square represents the activity of the pre-equilibrated enzyme at *p*H 6.8 in the presence of 0.5 m*M* ATP.

and that the degree of inhibition depended on enzyme polymerization state (Fig. 4B). When trehalase was predominately polymerized, the enzyme was far more sensitive to ATP inhibition [inhibition constant (K_i) = 0.17 m*M*] than was the dissociated form (K_i = 0.91 m*M*). Under these conditions, the more polymerized form also exhibited a higher Michaelis constant (K_m) for trehalose (34.4 m*M*), compared to a value of 16.4 m*M* for the lower molecular weight form. Although the differences in the K_m emphasize that the assembly states of trehalase are kinetically distinct, both forms are probably saturated by substrate in vivo because the trehalose level in hydrated cysts was 327 ± 8 (SEM) m*M* (*15*). However, at this physiological substrate level the polymerized enzyme did exhibit 14 percent substrate inhibition, which was not seen with the dissociated form.

On the basis of our in vitro evidence, the hysteretic assembly of trehalase into an aggregated form may explain the *p*H-induced arrest of trehalose mobilization in *Artemia* embryos and, consequently, the shutdown of metabolism observed during anaerobic dormancy and aerobic acidosis. When the enzyme is in the polymerized state fostered by acidic *p*H, it is virtually inactive under physiological conditions (*p*H 6.8, 0.5 m*M* ATP, and 320 m*M* trehalose) (Fig. 3, closed square). This ATP concentration is conservative because it approximates the lowest level we have measured in cysts under either of the quiescent states (*7*).

When interconversion of a hysteretic enzyme involves association and dissociation of subunits, one polymerization state is usually catalytically active and the other inactive. Well-known examples include glycogen phosphorylase (*16*), acetyl coenzyme A (CoA) carboxylase (*17*), and phosphofructokinase (PFK) (*13, 18*). Our data show that hysteretic interconversion of *Artemia* trehalase is an unusual mode of regulation for this enzyme because the interconversion occurs between two catalytically active assembly states that differ in kinetic properties.

Considerable attention has been directed to cyclic adenosine 3′, 5′-monophosphate (cAMP)–dependent activation of trehalase in dormant fungal spores. Glucose and heat activation of spores (*19*) or membrane-depolarizing agents (*20*) stimulate a transient increase in cAMP and a sudden tenfold rise in trehalase activity (*19–21*). Trehalase activation also can be elicited in crude extracts by providing all conditions necessary for cAMP-induced protein phosphorylation (*22*). We have been unable to obtain evidence for a similar cAMP-mediated activation of trehalase from *Artemia* embryos using comparable techniques. Incubation of embryo extracts with various levels of ATP, cAMP, and the catalytic subunit of beef heart protein kinase (with and without phosphodiesterase and phosphatase inhibitors) had no effect on trehalase activity.

Thus, the mechanism for *p*H-dependent trehalase regulation in brine shrimp embryosis apparently distinct from phosphorylation-based processes, and its hysteretic nature may offer certain advantages for controlling the shutdown of energy metabolism. A hysteretic enzyme at the control point of trehalose utilization could buffer the response time of this pathway to minor or short-term fluctuations in pH_i, which otherwise could be unnecessarily disruptive to routine metabolism. The buffering capacity would be dependent on the halftime for enzyme interconversion (*9*). In addition, the assembly-based mechanism provides a great deal of flexibility in the control of trehalase activity with little expenditure of chemical energy, a feature that could be particularly important for a cryptobiotic organism undergoing numerous bouts of environmentally induced dormancy during its development.

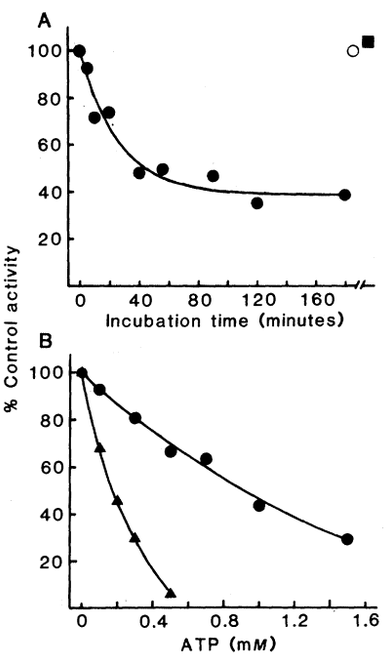

Fig. 4. (A) Hysteretic inhibition of trehalase activity upon titration of the enzyme at time zero from *p*H 8.6 to 6.3 (closed circles). Open circle indicates activity of control (nontitrated) enzyme at the end of the experimental time course. Closed square shows the restoration of activity in a titrated sample upon returning the *p*H to 8.6 by dialysis. Assays were performed at *p*H 7.0. (B) Inhibition of trehalase activity by ATP. Closed circles are the inhibition of the enzyme dialyzed at *p*H 8.6 and assayed (without pre-equilibration) at *p*H 6.8. Triangles represent the ATP inhibition observed for enzyme pre-equilibrated at *p*H 6.8 for 4 hours prior to catalytic measurements at that same *p*H.

REFERENCES AND NOTES

1. W. B. Busa and R. Nuccitelli, *Am J. Physiol.* **246**, R409 (1984).
2. J. Dutrieu and D. Chrestia-Blanchine, *C. R. Acad. Sci. Ser. D.* **263**, 998 (1966); R. D. Ewing and J. S. Clegg, *Comp. Biochem. Physiol.* **31**, 297 (1969).
3. W. B. Busa *et al.*, *Arch. Biochem. Biophys.* **216**, 711 (1982).
4. W. B. Busa and J. H. Crowe, *Science* **221**, 366 (1983).
5. D. N. Emerson, *Proc. S. D. Acad. Sci.* **42**, 131 (1963).
6. J. S. Clegg, *J. Exp. Biol.* **41**, 879 (1964).
7. J. C. Carpenter and S. C. Hand, *J. Comp. Physiol.*, in press.
8. B. Chance *et al.*, *Nature (London)* **182**, 1190 (1958).
9. C. Frieden, *J. Biol. Chem.* **245**, 5788 (1970); ———, *Annu. Rev Biochem.* **40**, 653 (1971).
10. The 7% acrylamide gels were prepared in 83 m*M* imidazole-HCl buffer (*p*H 7.8) without a stacking gel and electrophoresed (3 mA per gel) at 4°C in a reservoir buffer (*p*H 7.0) containing 30 m*M* diethylbarbituric acid and 3.36 m*M* imidazole. A maximum of 50 minutes was required for each run. Gels were stained for trehalose-dependent activity by incubating at 30°C for 1 to 3 hours in 0.1*M* tricine-NaOH buffer (*p*H 7.8) with trehalose (0.5*M*) glucose oxidase (12 units per milliliter), phenazine methosulfate (0.06 mg/ml), nitroblue tetrazolium (0.24 mg/ml), and $MgCl_2$ (2 m*M*). Incubation in the same mixture, but with trehalose omitted, resulted in no enzyme staining pattern.
11. S. Friedman and S. Alexander, *Biochem. Biophys. Res. Commun.* **42**, 818 (1971); K. A. Killick, *Exp. Mycol.* 7, 66 (1983).
12. Cysts were hydrated in tap water at 4°C for 4 hours and then homogenized in 3 volumes of 0.25*M* sucrose containing 1.0 m*M* phenylmethylsulfonyl fluoride (PMSF). After sequential centrifugations at 1000*g* (10 minutes) and 15,000*g* (20 minutes), the supernatant was neutralized by adding sodium phosphate buffer (50 m*M* final concentration) and fractionated with ammonium sulfate. The fraction precipitating between 40 and 80% saturation with $(NH_4)_2SO_4$ was collected by centrifugation, dialyzed against chromatography buffer (50 m*M* phosphate, *p*H 7.0, with 0.1 m*M* PMSF), and applied to a hydroxylapatite column. Trehalase activity could be eluted from the column with both 50 m*M* and 200 m*M* phosphate buffer, the two fractions differing in the proportion of trehalase forms present.
13. S. C. Hand and J. F. Carpenter, *Am J. Physiol.* **250**, R505 (1986); J. F. Carpenter and S. C. Hand, *ibid.*, p. R512.
14. Trehalase activity was routinely assayed at 30°C in a 0.5-ml reaction mixture containing 80 m*M* tricine, 80 m*M* citrate, 330 m*M* trehalose, 1 m*M* PMSF, 1.6 m*M* $MgCl_2$, and 0 to 0.1 ml enzyme. After 5 minutes of incubation, the reaction was stopped by a 5-minute exposure to 100°C. The glucose produced was analyzed by the glucose oxidase procedure [H. U. Bergmeyer and E. Bernt, in *Methods in Enzymatic Analysis*, H. U. Bergmeyer, Ed. (Academic Press, New York, 1974), p. 1205].
15. Trehalose concentration in cysts hydrated in 0.25*M* NaCl was determined with the anthrone method (*7*). The resulting value of 0.181 ± 0.004 (SEM) moles of trehalose per kilogram of hydrated cysts was then divided by the water content [0.553 ± 0.002 (SEM) liters per kilogram of hydrated cysts, equilibrated with 0.25*M* NaCl; calculated from J. S. Clegg, *J. Exp. Biol.* **61**, 291 (1974)].
16. B. Metzger *et al.*, *Biochemistry* 7, 2021 (1968).
17. C. Gregolin *et al.*, *Proc. Natl. Acad. Sci. U.S.A.* **56**, 1751 (1966).
18. P. E. Bock and C. Frieden, *J. Biol. Chem.* **251**, 5630 (1976); *ibid.*, p. 5637.
19. J. M. Thevelein *et al.*, *J. Gen. Microbiol.* **129**, 719 (1983); R. M. Van Mulders and A. J. Van Laere, *ibid.* **130**, 541 (1984).
20. J. M. Thevelein *et al.*, *J. Bacteriol.* **158**, 337 (1984).
21. J. A. Van Assche *et al.*, *Planta* **103**, 327 (1972); J. M. Thevelein *et al.*, *Proc. Natl. Acad. Sci. U.S.A.* **79**, 3503 (1982).
22. A. J. Van Laere and P. Hendrix, *J. Gen. Microbiol.* **129**, 3287 (1983).

23. We thank the National Science Foundation for support of this work through grant DCB-8316711.

16 December 1985; accepted 25 February 1986